

# A multiple model approach to respiratory motion prediction for real-time IGRT

Putra, D. , Haas, O.C.L. , Mills, J.A. and Burnham, K.

**Author post-print (accepted) deposited in CURVE May 2012**

**Original citation & hyperlink:**

Putra, D. , Haas, O.C.L. , Mills, J.A. and Burnham, K. (2008) A multiple model approach to respiratory motion prediction for real-time IGRT. *Physics in Medicine and Biology*, volume 53 (6): 1651.

<http://dx.doi.org/10.1088/0031-9155/53/6/010>

**Copyright © and Moral Rights are retained by the author(s) and/ or other copyright owners. A copy can be downloaded for personal non-commercial research or study, without prior permission or charge. This item cannot be reproduced or quoted extensively from without first obtaining permission in writing from the copyright holder(s). The content must not be changed in any way or sold commercially in any format or medium without the formal permission of the copyright holders.**

**This document is the author's post-print version, incorporating any revisions agreed during the peer-review process. Some differences between the published version and this version may remain and you are advised to consult the published version if you wish to cite from it.**

**CURVE is the Institutional Repository for Coventry University**

<http://curve.coventry.ac.uk/open>

# A multiple model approach to respiratory motion prediction for real-time IGRT

Devi Putra<sup>1</sup>, Olivier C L Haas<sup>1</sup>, John A Mills<sup>2</sup>, Keith J Burnham<sup>1</sup>

<sup>1</sup> Control Theory and Applications Centre, Coventry University, Priory Street, Coventry CV1 5FB, United Kingdom.

<sup>2</sup> Arden Cancer Centre, University Hospitals Coventry and Warwickshire, Coventry CV2 2DX, United Kingdom.

E-mail: [devi.putra@coventry.ac.uk](mailto:devi.putra@coventry.ac.uk), [o.haas@coventry.ac.uk](mailto:o.haas@coventry.ac.uk), [john.mills@uhcw.nhs.uk](mailto:john.mills@uhcw.nhs.uk) and [k.burnham@coventry.ac.uk](mailto:k.burnham@coventry.ac.uk).

## Abstract.

Respiration induces significant movement of tumours in the vicinity of thoracic and abdominal structures. Real-time image-guided radiotherapy (IGRT) aims to adapt radiation delivery to tumour motion during irradiation. One of the main problems for achieving this objective is the presence of time lag between the acquisition of tumour position and the radiation delivery. Such time lag causes significant beam positioning errors and affects the dose coverage. A method to solve this problem is to employ an algorithm that is able to predict future tumour position from available tumour position measurements. This paper presents a multiple model approach to respiratory-induced tumour motion prediction using the interacting multiple model (IMM) filter. A combination of two models, constant velocity (CV) and constant acceleration (CA), are used to capture respiratory-induced tumour motion. A Kalman filter is designed for each of the local models and the IMM filter is applied to combine the predictions of those Kalman filters for obtaining predicted tumour position. The IMM filter, likewise the Kalman filter, is a recursive algorithm that it is suitable for real-time applications. In addition, this paper proposes a confidence interval (CI) criterion to evaluate the performance of tumour motion prediction algorithms for IGRT. The proposed CI criterion provides a relevant measure for the prediction performance in terms of clinical applications and can be used to specify the margin to accommodate prediction errors. The prediction performance of the IMM filter has been evaluated using 110 traces of 4-minute free-breathing motion collected from 24 lung-cancer patients. The simulation study was carried out for prediction time 0.1-0.6 s with sampling rates 3, 5 and 10 Hz. It was found that the prediction of the IMM filter was consistently better than the prediction of the Kalman filter with CV or CA model. There was no significant difference of prediction errors for the sampling rates 5 and 10 Hz. For these sampling rates the errors of the IMM filter for 0.4 s prediction time were less than 2.1 mm in terms of the 95% CI criterion or 1.1 mm in terms of standard deviation (SD) or root mean squared errors (RMSE) criterion. For the prediction time 0.6 s the errors were less than 3.6 mm in terms of the 95% CI criterion or 1.8 mm in terms of SD/RMSE criterion. The prediction error analysis showed that the average percentage of the target lies outside the 95% CI margin was 5.2% and outside the SD/RMSE margin was 24.3%. This indicates the effectiveness of the 95% CI criterion as a margining strategy to accommodate prediction errors.

Submitted to: *Phys. Med. Biol.*

## 1. Introduction

Real-time image-guided radiotherapy (IGRT) aims to adapt the radiation delivery to tumour motion during a treatment session based on the information provided by an imaging system. Such images can be obtained from, for example, X-ray fluoroscopy imaging (Shirato et al., 2000; Seppenwoolde et al., 2002), electronic portal imaging (Berbeco et al., 2005a), external surrogate CCD camera imaging (Ozhasoglu and Murphy, 2002; George et al., 2005; Berbeco et al., 2005b) or a combination of them (Schweikard et al., 2000). Several methods for the implementation of real-time IGRT have been developed or are under development. Respiratory gating turns the radiation beam on (off) if a moving tumour is within (outside) a prescribed region of respiratory motion (Ohara et al., 1989; Kubo and Hill, 1996; Shirato et al., 2000; Keall et al., 2002). Tumour tracking continuously synchronises the radiation beam with a moving tumor during irradiation. Such synchronisation can be achieved, for example, by using dynamic multi-leaf collimators (MLC) (Keall et al., 2001; Neicu et al., 2003), a robotic manipulator (Schweikard et al., 2000) or a motorised patient support system (PSS) (D'Souza et al., 2005; Skworcow et al., 2007).

In both respiratory gating and tumour tracking systems, a time lag is present between the acquisition of tumour position and the radiation delivery. This time lag is due to image processing time, response time of the treatment machine and communication delay in the control loop. Shirato et al. (2000) report a time delay of 0.09 s between the time of the marker recognition and the start of irradiation in a gating system. Measurement results of Jin and Yin (2005) for a similar gating system show that the time lag including the response time of the linac and the delivery time is  $0.17 \pm 0.03$  s. In the robotic radiation delivery system studied in (Schweikard et al., 2000), the time lag including the response time of the robot is in the order of 0.3 s. Since the target position can be obtained with the rate from 30 Hz (Shirato et al., 2000) up to 60 Hz (Schweikard et al., 2000), this observation indicates that the main contributor to the time lag is the response time of the radiotherapy machines. The time lag causes a mismatch between the location of the radiation beam and the tumour due to the motion of the tumour during the time lag interval. Consequently, it results in underdosing to some parts of the target volume (Vedam et al., 2005).

To compensate the time lag some form of prediction method is required. Shirato et al. (2000) implement a linear extrapolation method to predict 0.09 s ahead tumour position and achieve prediction errors less than 1.5 mm. Murphy et al. (2002) propose an adaptive linear filter to predict tumour motion using a combination of internal and external markers measurements and show the effectiveness of the filter for prediction times up to 0.5 s using standard deviation (SD) criterion. The prediction performance of a linear filter, a Kalman filter and an artificial neural network (ANN) for different imaging rates and prediction times has been investigated in (Sharp et al., 2004). The

best predictor, ANN, achieved root mean squared errors (RMSE) less than 2 mm for prediction time 0.2 s with 30 Hz sampling rate. Vedam et al. (2004) compare the prediction performance of an adaptive sinusoidal filter and an adaptive linear filter. The adaptive linear filter performed better and achieved prediction errors less than 2 mm in terms of SD for prediction time less than 0.4 s with 10 Hz sampling rate. Isaksson et al. (2005) propose an adaptive ANN and show that its prediction performance is better than that of the adaptive linear filter in terms of the normalized RMSE. Furthermore, Murphy and Dieterich (2006) show that nonlinear ANN outperforms linear ANN in predicting irregular breathing motion.

All of the prediction methods mentioned above, except the sinusoidal filter of (Vedam et al., 2004), are non model-based approaches. Note that the Kalman filter of Sharp et al. (2004) is considered as non model-based because the matrices in the Kalman filter were obtained from the time series data. The aim of this paper is to propose a multiple model approach to tumour motion prediction using the interacting multiple model (IMM) filter algorithm and to compare its performance to a single model Kalman filter. The IMM filter, which is originally published in (Blom and Bar-shalom, 1988), has been successfully applied for aircraft tracking systems and our preliminary results in (Putra et al., 2006) show its potential for respiratory-induced tumour motion prediction. In addition, this paper proposes a confidence interval (CI) criterion to evaluate the performance of tumour motion prediction algorithms for IGRT. The advantages of the proposed CI criterion are that it provides information about target coverage, which is useful for treatment-plan evaluation, and it can be directly used to specify the margin to accommodate prediction errors. Since any prediction is subject to errors such a margin is necessary to ensure target coverage.

This paper is organized as follows. Section 2 describes the proposed methods including the multiple model approach, Kalman filter, the IMM algorithm and the CI criterion. The clinical data that is used to assess the filters performance is presented in section 3. Section 4 provides a discussion about the results. Finally, conclusions are given in section 5.

## **2. Methods**

### *2.1. Multiple model approach to respiratory motion*

To predict respiratory motion using Kalman filter and IMM algorithm, models for a short time evolution of the motion are required. Several models have been proposed to mimic respiratory-induced tumour motion, see for example (Lujan et al., 1999; Seppenwoolde et al., 2002; Wu et al., 2004; Sahih et al., 2005). This paper proposes a set of stochastic discrete-time linear models that are suitable to apply in the Kalman filter and the IMM algorithm.

A constant velocity (CV) model is proposed to capture segments of target trajectories where the target moves at almost constant velocities. The CV model is

given by

$$\begin{bmatrix} x_1(k) \\ x_2(k) \end{bmatrix} = \begin{bmatrix} 1 & \Delta t \\ 0 & 1 \end{bmatrix} \begin{bmatrix} x_1(k-1) \\ x_2(k-1) \end{bmatrix} + \begin{bmatrix} \frac{\Delta t^2}{2} \\ \Delta t \end{bmatrix} v(k-1) \quad (1)$$

$$y(k) = \begin{bmatrix} 1 & 0 \end{bmatrix} x(k) + w(k) \quad (2)$$

where  $x_1$  and  $x_2$  denote the position and the velocity of the target,  $\Delta t > 0$  is the sampling interval,  $y$  is the measured target position,  $v$  and  $w$  denote the process and measurement noises that are assumed to be uncorrelated zero-mean Gaussian white noises with variance  $Q$  and  $R$ , respectively. Note that the scalar process noise  $v$  in (1) behaves as a random acceleration/deceleration, which allows the changing of velocity direction, i.e. sign of  $x_2$ . The value of the process noise variance  $Q$  should be chosen to cover all possible rates of change of the velocity state  $x_2$ .

To capture segments of target trajectories where the target accelerates (decelerates) at almost constant accelerations (decelerations) a constant acceleration (CA) model is proposed. The CA model reads as

$$\begin{bmatrix} x_1(k) \\ x_2(k) \\ x_3(k) \end{bmatrix} = \begin{bmatrix} 1 & \Delta t & \frac{\Delta t^2}{2} \\ 0 & 1 & \Delta t \\ 0 & 0 & 1 \end{bmatrix} \begin{bmatrix} x_1(k-1) \\ x_2(k-1) \\ x_3(k-1) \end{bmatrix} + \begin{bmatrix} \frac{\Delta t^2}{2} \\ \Delta t \\ 1 \end{bmatrix} v(k-1) \quad (3)$$

$$y(k) = \begin{bmatrix} 1 & 0 & 0 \end{bmatrix} x(k) + w(k) \quad (4)$$

which is an extension of (1)-(2) by including the acceleration state denoted by  $x_3$ . Note that the scalar process noise  $v$  in (3), which acts as a random disturbance to the acceleration state  $x_3$ , is added to accommodate uncertainty in the estimated value of  $x_3$ . The value of the variance  $Q$ , in this case, should be chosen according to the magnitude of that uncertainty.

Respiratory-induced tumour motion exhibits quasi-periodic motion and some irregularities (Wu et al., 2004). During steady inhale and exhale phases, respiratory motion is almost at a constant velocity. At the transition between inhale and exhale, respiratory motion is decelerated at the end of inhale/exhale and is accelerated at the beginning of exhale/inhale. A single CV model or a single CA model may not be adequate to capture the dynamics of respiratory motion. For this reason, a hybrid combination of CV and CA models is proposed. Hybrid systems are characterised by multiple models that describe various behaviour modes, for further discussion on multiple model approach please refer to e.g. (Murray-Smith and Johansen, 1997). In each mode there is a ‘base state’ and a ‘modal state’. The ‘base state’ describes the local model dynamics and the ‘modal state’ indicates in what mode the system is at a certain time. Let rewrite (1)-(2) and (3)-(4) as

$$\xi_j(k) = F_j \xi_j(k-1) + G_j v_j(k-1) \quad (5)$$

$$y_j(k) = H_j \xi_j(k) + w_j(k) \quad (6)$$

where the index  $j = 1$  indicates the CV model,  $j = 2$  indicates the CA model and  $\xi_j = x$ . The proposed hybrid system is, then, described by the following three equations.

$$\xi(k) = \sum_{j=1}^2 \mu_j(k-1) (F_j \xi_j(k-1) + G_j v_j(k-1)) \quad (7)$$

$$y(k) = \sum_{j=1}^2 \mu_j(k-1) (H_j \xi_j(k-1) + w_j(k-1)) \quad (8)$$

$$\mu(k) = \Pi^T \mu(k-1) \quad (9)$$

where  $\mu$  is the modal state with its element  $\mu_j \in [0, 1]$  the probability being in mode  $j$  and  $\Pi$  is a  $2 \times 2$  Markovian transition matrix with its element  $\pi_{ij} \in [0, 1]$  the probability of the transition from being in mode  $i$  at time step  $k-1$  to being in mode  $j$  at time step  $k$  and  $\sum_{j=1}^2 \pi_{ij} = 1$  for  $i = 1, 2$ . Since  $\mu$  can take any value between 0 and 1 the hybrid system allows soft switching between the local models. Notice that the CV model has two states whilst the CA models has three states. In order to make the representation (7) and (8) proper the CV model (1)-(2) is extended to have three states where the third

state is set to zero, i.e. set  $F_1 = \begin{bmatrix} 1 & \Delta t & 0 \\ 0 & 1 & 0 \\ 0 & 0 & 0 \end{bmatrix}$ ,  $G_1 = \begin{bmatrix} \frac{\Delta t^2}{2} \\ \Delta t \\ 0 \end{bmatrix}$  and  $H_1 = [1 \ 0 \ 0]$ .

Note that the above CV and CA models and their hybrid combination are proposed to capture dynamics in 1-dimensional respiratory motion. By assuming that the dynamics in each dimension is independent, 3-dimensional (3D) respiratory motion can be modelled by having 3 models in parallel, i.e. one model for each dimension.

## 2.2. Kalman filter

The Kalman filter is an optimal state estimator for linear systems, e.g. CV and CA models, which minimizes the mean of the squared estimation error (Kalman, 1960). The recursive feature of Kalman filter makes it suitable for online prediction. It has been widely used for target tracking and autonomous navigation. The Kalman filter algorithm consists of prediction and update steps, for details see the filtering step of the IMM algorithm and (Kalman, 1960; Welch and Bishop, 1995).

The standard Kalman filter algorithm provides one-sample ahead prediction. If, however,  $N$ -sample ahead predictions are required, the predicted target position can be modified to

- Predicted position:  $\hat{y}_j(k-1+n|k-1) = H_j \hat{\xi}_j(k-1+n|k-1)$ , for  $n = 1, 2, \dots, N$   
with  $\hat{\xi}_j(k-1+n|k-1) = F_j^n \hat{\xi}_j(k-1)$ ,

where  $\hat{y}_j(l+n|l)$  and  $\hat{\xi}_j(l+n|l)$  denote the predicted target position and the predicted state  $\xi_j$  at time step  $l+n$  given measurement up to time step  $l$  and  $\hat{\xi}_j(l)$  is the estimated state  $\xi_j$  after receiving the measurement at time step  $l$ .

In this paper, a Kalman filter is designed for each of the proposed CV and CA models. The Kalman filter with CV model is called Kalman CV and the one with CA model is called Kalman CA.

### 2.3. IMM filter

The IMM filter is a suboptimal state estimator for hybrid systems (switching linear systems), e.g. given by (7)-(9). The IMM filter uses a Kalman filter as the base state estimator for each of local models and utilizes the normalized likelihood of those Kalman filters to estimate the modal state. Likewise the Kalman filter, the IMM filter is a recursive filter, where each iterations consists of three steps. Let  $\mu_j(k|k-1)$  be the predicted probability for mode  $j$  at time step  $k$  given measurement up to time step  $k-1$ ,  $\mu_{i|j}(k|k-1)$  denote the mixing probability, i.e. the weight for the estimate of mode  $i$  at time step  $k-1$  for the initial condition of mode  $j$  for time step  $k$ ,  $\hat{\xi}_{0j}(k|k-1)$  and  $P_{0j}(k|k-1)$  denote the initial state and covariance of mode  $j$  for time step  $k$  after the interaction of all mode at time step  $k-1$  and  $\Lambda_j(k)$  denote the likelihood of mode  $j$  at time step  $k$ . For  $s$  local models, i.e.  $M_s = \{1, 2, \dots, s\}$ , the IMM algorithm reads as follows:

**(a)** Interaction ( $\forall i, j \in M_s$ )

- Mode probability prediction:  $\mu_j(k|k-1) = \sum_i \pi_{ij} \mu_i(k-1)$
- Mixing probability:  $\mu_{i|j}(k|k-1) = \pi_{ij} \mu_i(k-1) / \mu_j(k|k-1)$
- Initialization of local filters:  
 $\hat{\xi}_{0j}(k|k-1) = \sum_i \hat{\xi}_i(k-1) \mu_{i|j}(k|k-1)$   
 $P_{0j}(k|k-1) = \sum_i \{P_i(k-1) + [\hat{\xi}(k-1) - \hat{\xi}_{0j}(k|k-1)][\hat{\xi}(k-1) - \hat{\xi}_{0j}(k|k-1)]^T\} \times \mu_{i|j}(k|k-1)$

**(b)** Filtering [Kalman filter]( $\forall i, j \in M_s$ )

- Prediction:  $\hat{\xi}_j(k|k-1) = F_j \hat{\xi}_{0j}(k|k-1)$ ,  
 $P_j(k|k-1) = F_j P_{0j}(k|k-1) F_j^T + G_j Q_j G_j^T$ .
- Predicted target position (output):  $\hat{y}(k|k-1) = \sum_j H_j \hat{\xi}_j(k|k-1) \mu_j(k-1)$ .
- Residual:  $r_j(k) = y(k) - H_j \hat{\xi}_j(k|k-1)$ ,  $S_j(k) = H_j P_j(k|k-1) H_j^T + R_j$ .
- Kalman gain:  $K_j(k) = P_j(k|k-1) H_j^T S_j(k)^{-1}$ .
- Update:  $\hat{\xi}_j(k) = \hat{\xi}_j(k|k-1) + K_j(k) r_j(k)$ ,  
 $P_j(k) = P_j(k|k-1) - K_j(k) S_j(k) K_j(k)^T$ .
- Likelihood (Gaussian):  $\Lambda_j(k) = \frac{1}{\sqrt{2\pi S_j(k)}} \exp(-\frac{r_j(k)^2}{2S_j(k)})$ .
- Mode probability:  $\mu_j(k) = \frac{1}{\sum_i \Lambda_i(k) \mu_i(k|k-1)} \Lambda_j(k) \mu_j(k|k-1)$

**(c)** Combination ( $\forall i, j \in M_s$ )

$$\hat{\xi}(k) = \sum_j \hat{\xi}_j(k) \mu_j(k), \quad P(k) = \sum_j \{P_j(k) + [\hat{\xi}_j(k) - \hat{\xi}(k)][\hat{\xi}_j(k) - \hat{\xi}(k)]^T\} \mu_j(k).$$

The above IMM algorithm describes one-sample ahead prediction. Similarly to the Kalman filter, if  $N$ -sample ahead predictions are required, the prediction in the filtering step can be modified to:

- n-sample ahead predictions:  $\hat{y}(k-1+n|k-1) = \sum_j H_j \hat{\xi}_j(k-1+n|k-1) \mu_j(k-1)$ ,  
for  $n = 1, 2, \dots, N$  with  $\hat{\xi}_j(k-1+n|k-1) = F_j^n \hat{\xi}_{0j}(k|k-1)$ .

The IMM algorithm is initialized with the initial mode probability  $\mu(0) = \mu_0$  and each Kalman filter inside the IMM algorithm is initialized with  $\xi_j(0) = \xi_{j0}$  and  $P_j(0) = P_{j0}$ .

In this work, the IMM algorithm is implemented with two local filters: Kalman CV and Kalman CA. As in the multiple model representation, the extended CV model is applied in the Kalman CV in order to make the matrix operations in the IMM algorithm proper.

*2.4. Performance criteria*

Let the prediction error at time-step  $k$  be defined by

$$e(k) = y_{act}(k) - y_p(k|k - T_p) \tag{10}$$

where  $y_{act}(k)$  denotes the actual tumour position at time-step  $k$  and  $y_p(k|k - T_p)$  denotes the predicted tumour position at time-step  $k$  for given measurement up to time-step  $k - T_p$  with  $T_p$  is the prediction time horizon. Several criteria, which are summarised in Table 1, have been used to evaluate the performance of prediction algorithms for IGRT based on the error definition (2.4). (Vedam et al., 2004; Sharp et al., 2004; Putra et al., 2006; Isaksson et al., 2005; Murphy and Dieterich, 2006; Yan et al., 2006). Criteria to assess the prediction performance would be useful in terms of clinical applications if they could provide information for treatment-plan evaluation. In general, the criteria listed in Table 1 do not provide such information. Therefore, it is of interest to develop new criteria that satisfy this requirement.

Dose volume histogram (DVH) has been accepted as a tool for treatment-plan evaluation and can be used to compute tumour control probability (TCP) and normal tissue complication probability (NTCP) (Webb and Nahum, 1993; Kutcher and Burman, 1989). For a given dose profile, DVH is defined by target coverage (TC). Prediction errors is related to TC through the confidence interval (CI) of the errors. The CI of prediction errors provides information in terms of probability that the actual target position lies within a particular distance from the predicted position. A 95% CI of  $Y$  mm tells that for a given prediction  $y_p$  mm it is expected with 0.95 probability (confidence level) that the actual target position  $y_{act}$  lies within the interval  $[y_p - Y, y_p + Y]$ , i.e.  $P(y_p - Y \leq y_{act} \leq y_p + Y) = 0.95$ .

The CI criterion is derived from the distribution of the prediction error  $e$ . To illustrate the principle, let suppose the distribution of the error  $e$  can be approximated by a Gaussian distribution with mean  $\mu$  and standard deviation  $\sigma$ . The probability that

**Table 1.** Some criteria have been to evaluate prediction algorithms in radiotherapy

<b>Criteria</b>	<b>Formula</b>
Standard deviation (SD or $\sigma$ )	$\sqrt{\frac{1}{N} \sum_{k=1}^N (e(k) - \mu)^2}, \mu = \frac{1}{N} \sum_{k=1}^N e(k)$
Root mean squared errors (RMSE)	$\sqrt{\frac{1}{N} \sum_{k=1}^N e(k)^2}$
Nomalised root mean squared errors (nRMSE)	$\sqrt{\frac{\sum_{k=1}^N e(k)^2}{\sum_{k=1}^N (y_{act}(k) - \sum_{k=1}^N y_{act}(k))^2}}$
Mean absolute errors (MAE)	$\frac{1}{N} \sum_{k=1}^N  e(k) $

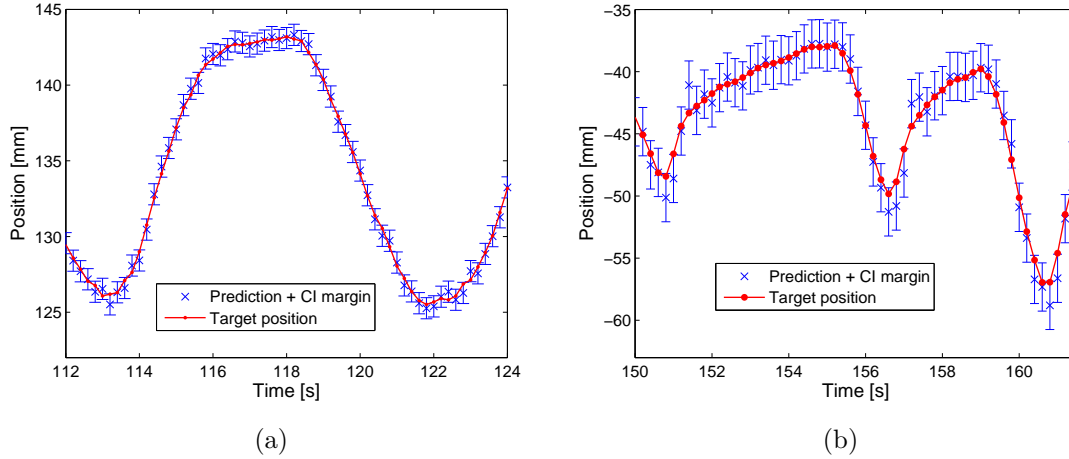


**Figure 1.** Illustration of using 95% CI criterion as margin to accommodate prediction errors of the IMM filter: regular motion (a) and irregular motion (b).

the error  $e$  lies within the interval  $[\mu - m\sigma, \mu + m\sigma]$  for a positive number  $m$  is given by

$$P(\mu - m\sigma \leq e \leq \mu + m\sigma) = \frac{1}{\sigma\sqrt{2\pi}} \int_{\mu - m\sigma}^{\mu + m\sigma} \exp\left(-\frac{(e - \mu)^2}{2\sigma^2}\right) de \quad (11)$$

$$= \frac{2}{\sqrt{\pi}} \int_0^{m/\sqrt{2}} \exp(-u^2) du = \text{erf}(m/\sqrt{2}), \quad (12)$$

where  $\text{erf}(\cdot)$  is called the erf function (Kenney and Keeping, 1962). For a given confidence level  $L$ , equation (12) allows calculation of the interval  $[\mu - m\sigma, \mu + m\sigma]$  defined by  $m = \sqrt{2}\text{erf}^{-1}(L)$ , where  $\text{erf}^{-1}$  denotes the inverse erf function. For example, the values of the parameter  $m$  for 68.3% and 95% confidence levels are equal to 1.00 and 1.96, respectively. The CI criterion, for a given confidence level, is defined by

$$\text{CI} = |\mu| + m\sigma. \quad (13)$$

Note that for  $\mu \neq 0$  the margin interval  $[\mu - m\sigma, \mu + m\sigma]$  is asymmetric, i.e. left margin is not equal to right margin, and the CI criterion takes the largest one. The CI criterion (13) takes into account systematic errors due to  $\mu$  as well as random errors due to  $\sigma$ .

From the definition of CI, the CI criterion (13) can be used to specify the margin needed to accommodate the prediction errors, see Figure 1 for illustrations. Furthermore, the confidence level of CI criterion can be adjusted to match a specific dose distribution objective. If the objective is, for example for a homogenous dose profile, to achieve 100% of the target volume receive at least 95% of the prescribed dose then the confidence level should be set to 95% (Putra et al., 2007). These advantages and the relation of CI to TC and DVH make the CI criterion suitable for assessing the performance of prediction algorithms for IGRT.

Note that SD criterion listed in Table 1 can provide the certainty region, which is related to CI, only in the case  $\mu = 0$ , i.e. unbiased predictors. In this case, SD criterion is the same as RMSE and the 68.4% CI criteria, see Table 1 and equation (13).

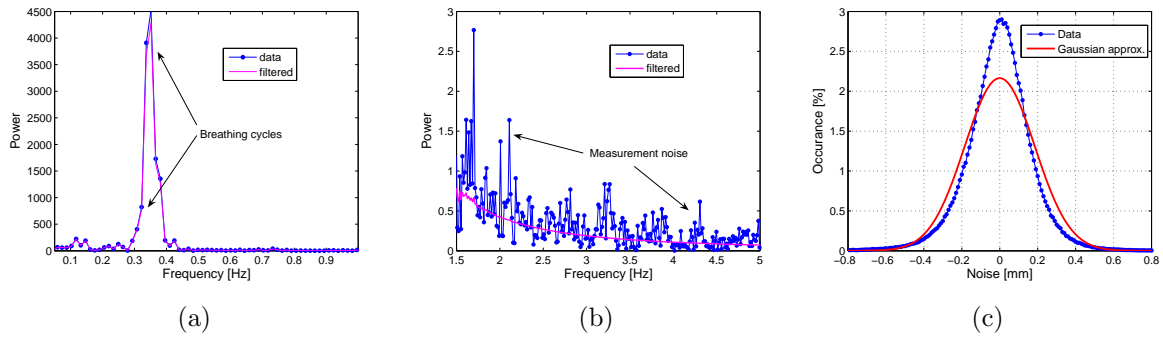


**Figure 2.** Breathing traces characteristics: power spectrum for lower frequencies (a) and for higher frequencies (b), and measurement noise histogram (c).

### 3. Material and analysis of measurement noise

The data, which are used to evaluate the prediction performance of the IMM and Kalman filters, consist of 110 traces of 4-minute free-breathing motion collected from 24 lung-cancer patients (George et al., 2005). The respiratory motion traces, which have 30 Hz sampling frequency, were acquired using the real-time position management (RPM) system of Varian Medical Systems, Palo Alto, California. The RPM system optically tracked the anterior-posterior motion of a reflective marker block, which was placed on the patient’s abdomen midway between the umbilicus and xyphoid process.

To analyse measurement noise contained in the breathing data a non-causal filter (filtfilt) is implemented in the Matlab software package (MathWorks, 2006) using a 3rd-order Chebyshev filter. The Chebyshev filter is designed to have 0.3 dB peak-to-peak ripple gain and 1.5 Hz cut-off frequency. The power spectrum plots in Figure 2 indicate that the Chebyshev filter is able to remove the measurement noise of the imaging system without distorting the breathing motion dynamics. The main frequencies of the breathing cycles are between 0.3 Hz and 0.4 Hz.

Having the filtered data  $y_f$ , the measurement noise  $\omega$  can be subtracted from the data  $y$  using the relation  $\omega = y - y_f$ . The histograms depicted in Figure 3 show that the distribution of the measurement noise can be well approximated by a Gaussian distribution with mean  $\mu = 0.00$  mm and standard deviation  $\sigma = 0.16$  mm. This validates the Gaussian assumption made in the CV and CA model, which is required by the Kalman and IMM filters. The noise analysis suggests that the actual target position should be given by the filtered data. Therefore, in this work the filtered data are used as the reference for computing the prediction errors instead of the measured data.

### 4. Results and discussion

Simulation studies using the clinically recorded breathing traces are carried out to evaluate the prediction performance of the proposed IMM, Kalman CV and Kalman CA filters. The prediction performance is evaluated for several prediction time horizons

and sampling rates. To obtain different sampling rates the original breathing data, which was sampled at 30 Hz sampling rate, are re-sampled. In this case, three sampling rates have been selected, namely: 3, 5 and 10 Hz. The prediction time horizon ranges from 0.1 s up to 0.6 s. The prediction times are chosen to be multiple of the sampling interval such that they can be formulated as  $N$ -step ahead predictions for some integer number  $N$ . The prediction error is computed using the filtered data as the actual target position, i.e.  $y_{act} = y_f$ . The filtering is carried out for the original 30 Hz sampling rate and the filtered data are re-sampled in the same way as the measured data. Hence, the prediction error (10) can be rewritten as  $e(k) = y_f(k) - y_p(k|k - N)$ , where  $N$  is the prediction time  $T_p$  in steps, i.e.  $T_p = N \times \Delta t$  with  $\Delta t$  the sampling interval. Note that the input to the prediction algorithms is the noisy (original) data  $y$ .

The design parameters of Kalman CV, Kalman CA and IMM filters are fixed for the whole simulations. They are obtained by means of manual tuning to minimise the 95% CI criterion following the guidance given in section 2.1. The process noise variance of Kalman CV and Kalman CA are set to  $Q_1 = 10 \text{ cm}^2\text{s}^{-4}$  and  $Q_2 = 1 \text{ cm}^2\text{s}^{-4}$  (the breathing data are in cm), respectively, while their measurement noise variance are set to  $R_1 = R_2 = 9 \times 10^{-4} \text{ cm}^2$ , respectively. The same designed parameters of Kalman CV and Kalman CA are used within the IMM algorithm and the Markovian transition matrix is set to  $\Pi = \begin{bmatrix} 0.9 & 0.1 \\ 0.2 & 0.8 \end{bmatrix}$ . This Markovian transition matrix assumes that the IMM filter is more frequently in the CV mode. The Kalman CV filter is initialized with  $\xi_{10} = [x_{10} \ x_{20}]^T$  where  $x_{10} = y(1)$  and  $x_{20} = (y(2) - y(1))/\Delta t$  with  $y(1)$  and  $y(2)$  are the first two measurements and  $\Delta t$  is the sampling interval, and  $P_{10} = I_{2 \times 2}$  where  $I$  denotes the identity matrix. The Kalman CA filter is initialized with  $\xi_{20} = [x_{10} \ x_{20} \ x_{30}]^T$  where the initial acceleration  $x_{30} = ((y(3) - y(2))/\Delta t - x_{20})/\Delta t$  and  $P_{20} = I_{3 \times 3}$ . The mode probability of the IMM filter is initialized with  $\mu(0) = [0.5 \ 0.5]^T$  meaning that there is no a priori knowledge about the mode probability.

The 95% CI criterion is used to evaluate the prediction performance of the proposed respiratory motion prediction algorithms. Prediction performances in terms of SD, RMSE and MAE are also provided to compare the appropriateness of the CI performance criteria. Prediction performances of the IMM, Kalman CV and Kalman CA filters with 10, 5 and 3 Hz sampling rates are summarized in Tables 2, 3 and 4, respectively. Note that ‘No prediction’ in Tables 2-4 refers to using measurement only and assuming that the target remains at the same position during the prediction time horizon. SD and RMSE criteria are put in one column because their values are the same. This is because, as discussed in section 2.4, the mean values of the prediction errors are about zero.

The simulation results showed that the prediction performance of the IMM filter was consistently better than that of the Kalman CV and Kalman CA filters, except for the prediction time 0.1 s with 10 Hz sampling rate where the prediction performance of the IMM and Kalman CV were equal. It was also found that the prediction performance of the Kalman CV was consistently better than that of the Kalman CA except for the prediction time 0.33 s with 3 Hz sampling rate where the prediction

**Table 2.** Prediction performance (mm) with 10 Hz sampling rate

Prediction method	Prediction time 0.1 s (N=1)			Prediction time 0.2 s (N=2)			Prediction time 0.3 s (N=3)		
	95% CI	SD/RMSE	MAE	95% CI	SD/RMSE	MAE	95% CI	SD/RMSE	MAE
IMM	0.49	0.25	0.19	0.92	0.47	0.35	1.44	0.74	0.54
Kalman CV	0.49	0.25	0.19	0.93	0.48	0.35	1.47	0.75	0.55
Kalman CA	0.53	0.27	0.20	1.04	0.53	0.40	1.71	0.87	0.65
No prediction	1.03	0.53	0.44	2.02	1.03	0.87	2.99	1.52	1.28

Prediction method	Prediction time 0.4 s (N=4)			Prediction time 0.5 s (N=5)			Prediction time 0.6 s (N=6)		
	95% CI	SD/RMSE	MAE	95% CI	SD/RMSE	MAE	95% CI	SD/RMSE	MAE
IMM	2.05	1.04	0.76	2.72	1.42	1.00	3.48	1.77	1.26
Kalman CV	2.09	1.07	0.76	2.78	1.42	1.00	3.55	1.81	1.27
Kalman CA	2.52	1.29	0.94	3.48	1.77	1.27	4.60	2.35	1.67
No prediction	3.94	2.01	1.69	4.88	2.48	2.09	5.79	2.95	2.48

**Table 3.** Prediction performance (mm) with 5 Hz sampling rate

Prediction method	Prediction time 0.2 s (N=1)			Prediction time 0.4 s (N=2)			Prediction time 0.6 s (N=3)		
	95% CI	SD/RMSE	MAE	95% CI	SD/RMSE	MAE	95% CI	SD/RMSE	MAE
IMM	0.91	0.46	0.35	2.08	1.05	0.77	3.57	1.80	1.31
Kalman CV	0.94	0.48	0.36	2.11	1.07	0.77	3.63	1.85	1.34
Kalman CA	1.02	0.52	0.38	2.44	1.25	0.89	4.46	2.27	1.59
No prediction	2.02	1.03	0.86	3.95	2.01	1.69	5.79	2.95	2.48

**Table 4.** Prediction performance (mm) with 3 Hz sampling rate

Prediction method	Prediction time 0.33 s (N=1)			Prediction time 0.67 s (N=2)		
	95% CI	SD/RMSE	MAE	95% CI	SD/RMSE	MAE
IMM	1.75	0.88	0.64	4.52	2.27	1.60
Kalman CV	2.00	1.02	0.78	4.60	2.34	1.73
Kalman CA	1.93	0.98	0.69	5.35	2.73	1.86
No prediction	3.28	1.67	1.41	6.36	3.24	2.73

performance of Kalman CV is worse than the performance of Kalman CA. Nevertheless, the prediction performance of the three proposed filters were always better than that of using measurements only, i.e. no prediction. These simulation results indicate that the IMM filter is able to combine the Kalman CV and Kalman CA filters to improve the prediction performance. The results in Tables 2-3 also show that the longer the prediction time the larger the difference between the performance of the IMM filter and that of the Kalman CV and Kalman CA filters. This suggests that the IMM filter performs much better than Kalman CV or Kalman CA filters for relatively longer prediction time. Examples of the IMM filter predictions can be seen in Figure 1.

Note that in this work the proposed Kalman CV, Kalman CA and IMM filters are used to predict respiratory motion because respiratory motion traces are used as the input data to the filters. However, the proposed filters can be used to predict tumour motion if the internal tumour motion data, e.g. as reported in (Shirato et al., 2000; Seppenwoolde et al., 2002), are available.

The following provides a discussion on the performance criteria. As shown in Tables 2-4, the 95% CI criterion always gives the largest measure for the prediction errors of all

**Table 5.** Percentage of target lies outside the performance criteria margin for the IMM filter prediction

Performance criteria	Sampling rate										
	10 Hz						5 Hz			3 Hz	
	Prediction time [s]						Prediction time [s]			Prediction time [s]	
	0.1	0.2	0.3	0.4	0.5	0.6	0.2	0.4	0.6	0.33	0.67
95% CI	4.8	4.5	4.8	5.1	5.6	6.1	4.4	4.6	5.3	5.6	6.0
SD/RMSE	27.2	25.9	24.2	23.8	22.0	22.1	26.0	25.2	24.3	23.4	23.0
MAE	39.5	39.9	39.2	37.7	36.3	35.9	39.9	39.0	37.4	35.9	34.8

prediction methods whilst the MAE criterion always gives the smallest one. However, all of the criteria give almost the same rank for the predictors performance, except for two cases as shown in Table 2. For the prediction time 0.4s, the MAE criterion gives the same rank (the first) for the IMM and Kalman CV filters whilst the 95% CI, SD and RMSE criteria give the first rank to the IMM filter and the second rank to the Kalman CV filter. However, for the prediction time 0.5s the MAE, SD and RMSE criteria give the same rank (the first) for the IMM and Kalman CV filters and only the 95% CI give the first rank to the IMM filter and the second rank to the Kalman CV filter. This indicates that the 95% CI performance criteria is more selective than the other criteria.

An illustration of the ability of the performance criteria to provide a relevant measure for the prediction errors in terms of target coverage is depicted in Table 5. The average of percentage of the target lies outside the 95% CI, SD/RMSE and MAE margin are 5.2%, 24.3% and 37.8%, respectively. The results confirms that the 95% CI criterion can be used as a margining strategy to accommodate prediction errors. It expects - and is confirmed by the simulation results - that about 95% of the time the target lies within the 95%CI margin and hence is covered by the beam portal. In this case, SD, RMSE and MAE criteria will give overestimate measure for the prediction errors because the SD, RMSE and MAE margin will cover the target only about 76% and 62% of the time, respectively.

The importance of using a relevant criterion to evaluate the performance of prediction algorithms for IGRT is prompted by the following example. Suppose the proposed filters would be applied to an IGRT tracking system, which is equipped with tumour imaging devices having 5 Hz sampling rate. It is required that the prediction errors be less than 1.5 mm. According to Table 3, the prediction performance of the IMM, Kalman CV and Kalman CA filters is acceptable for the system latency up to only 0.2 s if the 95% CI criterion is used. However, if SD/RMSE criterion is used the prediction performance of these filters is acceptable for the system latency up to 0.4 s. Moreover, according to MAE criterion the prediction performance of the IMM and Kalman CV filters is acceptable for the system latency up to 0.6 s.

## 5. Conclusion

A multiple model approach to respiratory motion prediction using the IMM filter has been presented. The simulation study using 110 traces of 4-minute free-breathing motion from 24 lung-cancer patients showed that the prediction of the IMM filter with CV and CA models consistently outperformed the prediction of the Kalman filter with CV model (Kalman CV) or the Kalman filter with CA model (Kalman CA). However, the performance of the IMM, Kalman CV and Kalman CA filters were always better than using measurement only (no prediction). The results indicate that the IMM filter is preferable for relatively longer prediction time and slower sampling rate. For the sampling rate 5 Hz, the IMM filter was able to achieve prediction errors less than 2.1 mm in terms of the 95% CI criterion or 1.1 mm in terms of SD/RMSE criterion and for the prediction time 0.6 s the errors were less than 3.6 mm in terms of the 95% CI criterion or 1.8 mm in terms of SD/RMSE criterion.

The confidence interval (CI) criterion has been proposed to measure the performance of prediction algorithms for IGRT. The confidence level of the CI criterion can be adjusted to meet a specific dose distribution objective. It has been shown that the 95% CI criterion provides more relevant measure for the prediction performance in terms of target coverage compared to SD, RMSE and MAE criteria. The simulation results confirmed that the proposed 95% CI criterion can be used to specify the margin to accommodate prediction errors. The results showed that for the IMM filter predictions the maximum percentage of the target lies outside the 95% CI margin was 6.1% whilst outside the SD/RMSE and MAE margin were 27.2% and 39.9%, respectively.

## Acknowledgments

This work is sponsored by the Framework 6 European integrated project Methods and Advanced Equipment for Simulation and Treatment in Radiation Oncology (MAESTRO) CE LSHC CT 2004 503564. The Authors are grateful to the Department of Radiation Oncology, Virginia Commonwealth University, USA for providing the data used in this manuscript.

## References

- R.I. Berbeco, T. Neicu, E. Rietzel, G.T. Chen, and S.B. Jiang. A technique for respiratory-gated radiotherapy treatment verification with an epid in cine mode. *Physics in Medicine and Biology*, 50:3669–3679, 2005a.
- R.I. Berbeco, S. Nishioka, H. Shirato, G.T.Y. Chen, and S.B. Jiang. Residual motion of lung tumours in gated radiotherapy with external respiratory surrogates. *Physics in Medicine and Biology*, 50:3655–3667, 2005b.
- H.A.P. Blom and Y. Bar-shalom. The interacting multiple model algorithm with

- markovian switching coefficients. *IEEE Transaction on Automatic Control*, 37(10): 780–783, 1988.
- W.D. D’Souza, S.A. Naqvi, and C.X. Yu. Real-time intra-fraction-motion tracking using the treatment couch: a feasibility study. *Physics in Medicine and Biology*, 50:4021–4033, 2005.
- R. George, S. S. Vedam, T. D. Chung, V. Ramakrishnan, and P. J. Keall. The application of the sinusoidal model to lung cancer patient respiratory motion. *Medical Physics*, 32(9):2850–2861, 2005.
- M. Isaksson, J. Jalden, and M.J Murphy. On using an adaptive neural network to predict lung tumour motion during respiration for radiotherapy applications. *Medical Physics*, 32:3801–3809, 2005.
- J. Jin and F. Yin. Time delay measurement for linac based treatment delivery in synchronized respiratory gating radiotherapy. *Medical Physics*, 32:1293–1296, 2005.
- R.E. Kalman. A new approach to linear filtering and prediction problems. *Transactions of the ASME - Journal of Basic Engineering*, 82:35–45, 1960.
- P.J Keall, V.R. Kini, S.S. Vedam, and R. Mohan. Motion adaptive x-ray therapy: a feasibility study. *Physics in Medicine and Biology*, 46:1–10, 2001.
- P.J Keall, V.R. Kini, S.S. Vedam, and R. Mohan. Potential radiotherapy improvements with respiratory gating. *Australas Phys. Eng. Sci. Med.*, 25:1–6, 2002.
- J.F. Kenney and E.S. Keeping. *Mathematics of Statistics*. Van Nostrand, 3 edition, 1962.
- H.D. Kubo and B.C. Hill. Respiration gated radiotherapy treatment: a technical study. *Physics in Medicine and Biology*, 41:83–91, 1996.
- G.J. Kutcher and C. Burman. Calculation of complication probability factors for non-uniform normal tissue irradiation: The effective volume method. *Int. J. Radiation Oncology Biol. Phys.*, 16:1623–1630, 1989.
- A.E. Lujan, E.W. Larsen, J.M. Balter, and R.K. Ten Haken. A method for incorporating organ motion due to breathing into 3d dose calculations. *Medical Physics*, 26(5), 1999.
- MathWorks. *Signal Processing Toolbox: For Use with MATLAB*. The MathWorks Inc., 2006.
- M.J Murphy and S. Dieterich. Comparative performance of linear and nonlinear neural networks to predict irregular breathing. *Physics in Medicine and Biology*, 51:5903–5914, 2006.
- M.J Murphy, J. Jalden, and M. Isaksson. Adaptive filtering to predict lung tumour breathing motion during image guided radiation therapy. In *the 16th International Congress on Computer-assisted Radiology and Surgery (CARS 2002)*, pages 539–544, 2002.
- J. Murray-Smith and T.A. Johansen. *Multiple Model Approaches to Modelling and Control*. Taylor and Francis, London, 1997.

- T. Neicu, H. Shirato, Y. Seppenwoolde, and S.B. Jiang. Synchronized moving aperture radiation therapy (SMART): average tumour trajectory for lung patients. *Physics in Medicine and Biology*, 48:587–598, 2003.
- K. Ohara, T. Okumura, T. Akisada, T. Inada, T. Mori, and H. Yokota and M.B. Calguas. Irradiation synchronize with respiration gate. *Int. J. Radiation Oncology Biol. Phys.*, 17:853–857, 1989.
- C. Ozhasoglu and M.J. Murphy. Issues in respiratory motion compensation during external-beam radiotherapy. *Int. J. Radiation Oncology Biol. Phys.*, 52:1389–1399, 2002.
- D. Putra, O.C.L. Haas, J.A. Mills, and K.J. Burnham. Prediction of tumour motion using interacting multiple model filter. In *Proceedings of the 3rd IET International Conference on Medical Signal and Information Processing (MEDSIP)*, 2006.
- D. Putra, P. Skworcow, K. Young, O.C.L. Haas, J.A. Mills, and K.J. Burnham. Margin to accommodate inherent errors of tracking-based radiation delivery system. In Jean-Pierre Bissonnette, editor, *XVth International Conference on the Use of Computers in Radiation Therapy, Toronto, Canada*, pages 190–194, June 2007.
- A. Sahih, O.C.L. Haas, K. Burnham, and J. Mills. Organ motion modelling and prediction for adaptive radiotherapy. In *IAR & ACD 2005*, pages 211–216, 2005.
- A. Schweikard, G. Glosser, M. Bodduluri, M. Murphy, and J.R. Adler. Robotic motion compensation for respiratory movement during radiosurgery. *Computer Aided Surgery*, 5:263–277, 2000.
- Y. Seppenwoolde, H. Shirato, K. Kitamura, S. Shimizu, M.V. Herkand J.V. Lebesque, and K. Miyasaka. Precise and real-time measurement of 3d tumour motion in lung due to breathing and heartbeat, measurement during radiotherapy. *Int. J. Radiation Oncology Biol. Phys.*, 53(4):822–834, 2002.
- G.C. Sharp, S.B. Jiang, S. Shimizu, and H. Shirato. Prediction of respiratory tumour motion for real-time image-guided radiotherapy. *Physics in Medicine and Biology*, 49:425–440, 2004.
- H. Shirato, S. Shimizu, T. Kunieda, K. Kitamura, M. van Herk and K. Kagei, T. Nishihoka, S. Hashimoto, K. Fujita, H. Aoyama and K. Tsuchiya, K. Kudo, and K. Miyasaka. Physical aspects of a real-time tumour tracking system for gated radiotherapy. *Int. J. Radiation Oncology Biol. Phys.*, 48:1187–1195, 2000.
- P. Skworcow, D. Putra, A. Sahih, J. Goodband, O.C.L. Haas and K.J. Burnham, and J.A. Mills. Predictive tracking for respiratory induced motion compensation in adaptive radiotherapy. *Measurement + Control*, 40(1):16–19, February 2007.
- S. Vedam, A. Docef, M. Fix, M. Murphy, and P. Keall. Dosimetric impact of geometric errors due to respiratory motion prediction on dynamic multileaf collimator-based four-dimensional radiation delivery. *Medical Physics*, 32(6), 2005.
- S.S. Vedam, P.J. Keall, A. Docef, D.A. Todor, and V.R. Kini and R. Mohan. Predicting

- respiratory motion for four-dimensional radiotherapy. *Medical Physics*, 31(8):2274–2283, 2004.
- S. Webb and A.E. Nahum. A model for calculating tumour control probability in radiotherapy including the effects of inhomogeneous distributions of dose and clonogenic cell density. *Physics in Medicine and Biology*, 38:653–666, 1993.
- G. Welch and G. Bishop. An introduction to the kalman filter. Technical Report TR 95-041, University of North Carolina at Chapel Hill (Online at <http://www.cs.unc.edu/welch/kalman/kalmanIntro.html>), 1995.
- H. Wu, G.C. Sharp, B. Salzberg, D. Kaeli, H. Shirato, and S.B. Jiang. A finite state model for respiratory motion analysis in image guided radiation therapy. *Physics in Medicine and Biology*, 49:5357–5372, 2004.
- H. Yan, F. Yin, G. Zhu, M. Ajlouni, and J.H. Kim. Adaptive prediction of internal target motion using external marker motion: a technical study. *Physics in Medicine and Biology*, 51:31–44, 2006.